Optical harmonics generation in metal/dielectric heterostructures in the presence of Tamm plasmon-polaritons

B. I. Afinogenov, A. A. Popkova, V. O. Bessonov, and A. A. Fedyanin

Faculty of Physics, Lomonosov Moscow State University, Moscow, 119991, Russia

ABSTRACT

We have studied an influence of Tamm plasmon-polaritons (TPPs) excitation on the nonlinear-optical response of one-dimensional photonic crystal/metal structures. It was shown that in case when the fundamental radiation is in resonance with the TPP, second-harmonic generation in the sample is enhanced over two times of magnitude in comparison with a bare metal film. Using methods of nonlinear transfer matrices it was demonstrated that the third-order nonlinear response of a metal/dielectric heterostructure, when both fundamental and third-harmonic radiation are in resonance with the first- and third-order TPPs respectively, can be enhanced via two mechanisms: fundamental field localization and optical harmonic resonant tunneling. The overall enhancement of the third harmonic generation in that case can exceed three orders of magnitude in comparison with the nonresonant case.

1. INTRODUCTION

Optical harmonics generation is a powerful tool which is widely used for noninvasive probing of buried interfaces[1] and living structures.[2,3] In bulk centrosymmetric materials generation of second optical harmonic is prohibited, however in atomic-thin layers near the boundaries it is allowed due to symmetry breaking. This allows for study properties of optically accessible interfaces with a very high accuracy, because no background signal presents. Intensity of second and third harmonics is proportional to fourth and sixth power of the fundamental electric field, respectively, thus the minor increase in a pump intensity results in a drastic increase in the nonlinear signal. Field enhancement can be realized in a several ways, e.g. by exciting localized or surface plasmons in metals,[4,5] or at the edge of a bandgap in dielectric photonic crystals (PCs).[6,7]

Tamm plasmon-polaritons (TPPs) are surface optical states, appearing as an electromagnetic field localization at an interface of a one-dimensional PC and metal film.[8] They can be observed experimentally as narrow resonances in transmission and reflection spectra of such structures,[9] and spectral position of resonance exhibits polarization splitting.[10] In contrast with surface plasmon-polaritons, TPPs can be excited by a direct optical illumination, and their excitation wavelength significantly depends on the angle of incidence.[9] TPPs can arise in conjunction with other excitations, such as microcavity modes,[11] excitons,[12] quantum dots[13] or surface plasmon-polaritons,[14] forming so-called hybrid states. Efficient energy transfer between components of these states allowed for creation of novel types of lasers, sensors, and integrated circuits.[15–17]

Enhancement of the electromagnetic field in PC/metal structure under conditions of Tamm plasmon-polariton excitation, leads to the increase in nonlinear-optical intensity at doubled and tripled frequency. Moreover, if TPP is excited at a sum frequency, harmonics intensity can exhibit resonant behavior due to tunneling through the TPP mode. Recently, it was proposed to construct double-resonance structure, which will benefit from both fundamental field localization and from harmonics radiation tunneling.[18] Previous studies on sum-frequency generation in photonic crystals supports the feasibility of an idea.[19]

In this paper the second and third optical harmonics generation enhancement in metal/dielectric structures in the presence of Tamm plasmon-polaritons is discussed. It was shown that the main channel of the SHG enhancement is the fundamental field localization in the TPP mode at the interface of metal and PC (resonant pump). For the third harmonic radiation a double resonant conditions can be fulfilled which results in pump field localization in the first-order TPP mode and increase in third-harmonic radiation transmission due to tunneling

Further author information: (Send correspondence to B.I.A)
B.I.A: E-mail: afinogenov@nanolab.phys.msu.ru

Photonic and Phononic Properties of Engineered Nanostructures VI, edited by Ali Adibi, Shawn-Yu Lin, Axel Scherer,
Proc. of SPIE Vol. 9756, 975611 · © 2016 SPIE · CCC code: 0277-786X/16/$18 · doi: 10.1117/12.2213337

through the third-order TPP mode. Numerical calculations by a nonlinear transfer matrix technique bolster experimental results.

2. THEORETICAL CONSIDERATIONS

Consider a structure arranged along z-axis, consisting of a semi-infinite photonic crystal laying at $z > 0$ with layers of thicknesses d_1, d_2 and dielectric constants $\varepsilon_1, \varepsilon_2$, and a metal with thickness d_{M} and a complex dielectric constant ε_{M}. As it was shown earlier,[14] the electric field in Tamm plasmon eigenmodes has the following form:

$$E(z) = \begin{cases} Ae^{-iqz}, & z < -d_{\mathrm{M}} \\ Be^{-\kappa_{\mathrm{M}} z} + Ce^{\kappa_{\mathrm{M}} z}, & -d_{\mathrm{M}} < z < 0 \\ Du(z)e^{iQz}, & z > 0 \end{cases}, \tag{1}$$

where A, B, C, D are complex constants, $q = \sqrt{k^2 - K^2}$, $\kappa_{\mathrm{M}} = \sqrt{K^2 - \varepsilon_{\mathrm{M}} k^2}$, K is a wavevector perpendicular to z, $k = \omega/c$, Q is a complex Bloch wavenumber, $u(z)$ is periodic with a period $\Lambda = d_1 + d_2$. Because $Q = \Lambda/\pi + iK_i$ is a complex number, the envelope of an electric field is an exponential decay function, and a maximum value of $E(z)$ is achieved at a center of the dielectric layer, adjacent to the metal. On the other hand, the nonlinear optical response of a medium is driven by a nonlinear polarization $\mathbf{P}^{NL}$, which have the form:

$$\mathbf{P}^{NL} = \hat{\chi}^{(2)}\mathbf{E}^2 + \hat{\chi}^{(3)}\mathbf{E}^3 + \ldots \quad . \tag{2}$$

It means that any field enhancement in a nonlinear medium leads to a consequent nonlinear polarization amplification. From equations (1) and (2) it can be concluded that if a dielectric layer with a non-zero nonlinear susceptibility is located close to the metal, the overall nonlinear optical response of structure in case of Tamm plasmon excitation is higher than in non-resonant case. Moreover, field at the metal boundary in metal/PC structure in case of TPP excitation is amplified in comparison to the field at the boundary of a bare metal film.

In case of second-harmonic generation, second-order polarization $P^{(2)}$ is proportional to the square of a fundamental electric field with a coefficient $\hat{\chi}^{(2)}$. In a bulk centrosymmetric medium, such as metal or fused dielectric, $\hat{\chi}^{(2)}$ is equal to zero due to inversion symmetry, however at several atomic layers near boundary of a material, where the symmetry is broken, second-order susceptibility has non-zero components. For a sample, comprising layers of SiO_2, Ta_2O_5 and silver, the second harmonic intensity is thus determined by a field at the inner silver boundary, because effective $\hat{\chi}^{(2)}_{\mathrm{Ag}} >> \hat{\chi}^{(2)}_{\mathrm{SiO_2,Ta_2O_5}}$.

In case of third-harmonic generation, contributions from all layers should be considered, because third-order susceptibility is non-zero for every layer in a structure. Third-order susceptibility $\hat{\chi}^{(3)}_{\mathrm{Ag}} \approx 10^3 \cdot \hat{\chi}^{(3)}_{\mathrm{SiO_2,Ta_2O_5}}$, but on the other hand, electric field has maximum enhancement in the top dielectric layer, adjacent to the metal, and the typical amplification factors are in the order of 5–10. From the equation (2) it can be seen that contributions from metal and dielectric layers are of the same order of magnitude in this case.

3. EXPERIMENTAL TECHNIQUES AND DATA

Two different sets of samples were prepared for the study using thermal evaporation and magnetron sputtering techniques. The first one (type1) is a $(SiO_2/Ta_2O_5)_7$ PC with average thicknesses of layers being 92 nm and 130 nm respectively, yielding a photonic bandgap between 650 nm and 920 nm under normal incidence. To allow for Tamm plasmon-polariton excitation, it was covered with a semitransparent 30-nm-thick silver film. Additionally, a 10-nm-thick Al_2O_3 layer was deposited atop silver to protect it from degradation due to contact with air. In first-type samples TPP resonant wavelength is around 820 nm at a normal incidence. Samples in the second set (type2) are heterostructures $(ABA^*B^*)_5$ where A stands for SiO_2 layers with thicknesses d_A = 240 nm, d_{A^*} = 284 nm, and B stands for Ta_2O_5 layers with thicknesses d_B = 164 nm, d_{B^*} = 194 nm. They were also covered with a 30-nm-thick silver film and a protective Al_2O_3 layer. At a 20° angle of incidence fundamental TPP resonance in type2 samples arises at 1550 nm and third-order TPP resonance is at 521 nm. Figure 1a shows a typical transmittance spectrum of type1 sample at a normal incidence. It exhibits a bandgap between 650 nm and 920 nm with a sharp peak at 820 nm inside it, which is associated with TPP resonance.

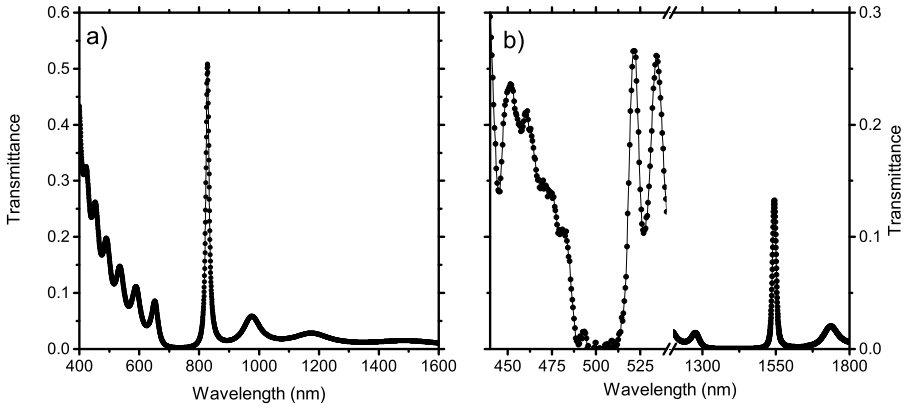

Figure 1. (Color online) a) Transmittance spectrum of type1 sample at normal incidence. b) Transmittance spectrum of type2 sample at 20° angle of incidence.

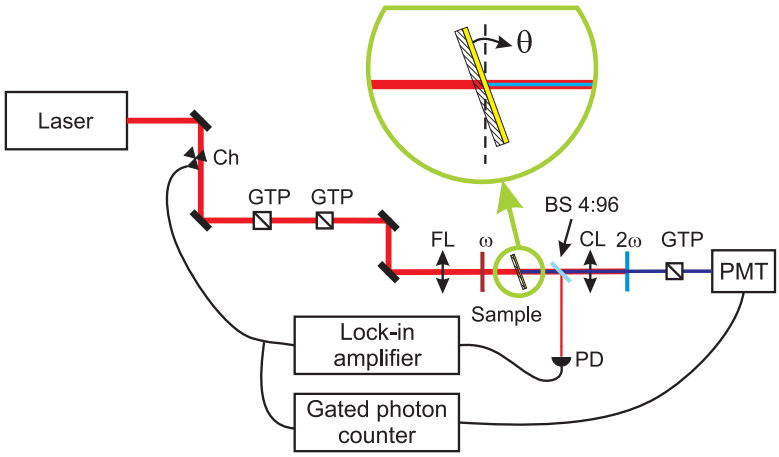

Figure 2. (Color online) Outline of the experimental setup. Ch is a chopper, GTPs are Glan-Taylor laser prisms, fixed in rotational mounts, FL is a focusing lens (fused silica, 50-mm focal length), ω denotes an optical filter, which transmits fundamental wavelength, but blocks two-photon luminescence from optical components of setup, Sample is mounted onto a rotational stage, allowing for precise control of an angle of incidence θ, beamsplitter BS is used to perform simultaneous measurements of a linear transmission (with a photodiode PD) and generated harmonics intensity (with a photomultiplier tube PMT), CL is a collimating lens (fused silica, 50-mm focal length), 2ω is a filter, passing radiation at harmonic frequency, but absorbing the fundamental one.

Resonant peculiarities are observed neither at 1550 nm nor at 400 nm. Transmittance spectrum of type2 sample at 20° angle of incidence is shown in Figure 1b. The first-order bandgap of sample is between 1250 nm and 1750 nm, while third-order bandgap lays between 460 nm and 530 nm. Tamm plasmon resonances present in both bandgaps, emerging at 1550 nm in fundamental one and at 520 nm in third-order one.

Outline of the setup used for studies is shown in Figure 2. A femtosecond laser is a source of radiation; two Glan-Taylor prisms, fixed in precise rotation mounts, are used to control power and polarization of fundamental radiation. It is then focused with a fused silica lens with 50-mm focal length, yielding approximately 40-μm-diameter spot in a focal plane. Sample is mounted onto an automated rotational stage, allowing for precise change of the angle of incidence, with a 0.01° angular accuracy of rotation. Radiation, transmitted through the sample is collimated in a confocal scheme, filtered at a harmonic wavelength, and analyzed with another Glan-Taylor prism. As a detector, a Hamamatsu PMT module, connected to a SRS gated photon counter was used. Coherent Chameleon laser, providing 130-fs pulses at 800 nm was used to perform measurements on type1 sample in case of resonant pump, and Avesta Project fiber laser with 200-fs pulses at 1560 nm was used in preliminary experiments on type2 samples.

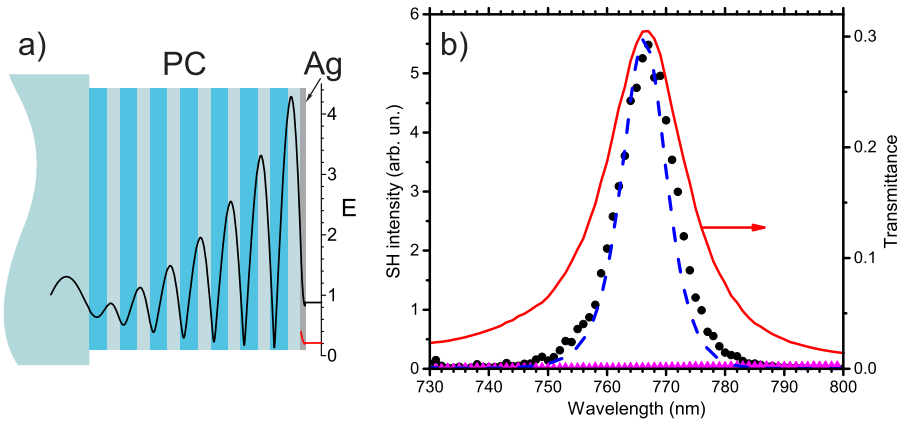

Figure 3. (Color online) a) Distribution of the electric field in PC/silver sample in case of TPP resonance (black curve). Distribution of electric field in a bare silver film (red curve). b) Intensity of the second-harmonic radiation, measured in a *pp*-geometry from PC/Ag sample (black circles) and a bare silver film (pink triangles). Transmittance of a fundamental radiation (solid red curve). Numerical calculations of the SH intensity, generated in sample (dashed blue curve).

3.1 Case of the resonant pump

Case of the resonant pump was explicitly explained in our previous study,[20] however we will summarize general ideas for clarity sake. The type1 sample is pumped by a laser, which central wavelength can be tuned between 700–800 nm, and PMT measures the signal at doubled frequency. Changing the laser wavelength allows for fundamental radiation to overlap with the TPP resonance. When the TPP resonance conditions are fulfilled, the electromagnetic field localization emerges at the PC/metal interface, as shown in Fig. 3a with a black curve. Field distribution peaks at approximately 4.5 in the PC layer, adjacent to the metal. Field enhancement in metal is 1.7 in comparison with the incident field, however in comparison with the field amplitude in a bare metal film (red curve in Fig. 3), the enhancement is significantly higher and reaches 4.3.

As it was mentioned earlier, in bulk centrosymmetric media second-harmonic generation is forbidden, thus the only sources of nonlinear polarization are atomic-thin layers at interfaces of structure layers. According to the previous studies, effective surface second-order susceptibility of silver is several orders of magnitude bigger than ones of dielectric layers, composing the sample, thus contribution from SH sources in dielectric layers can be neglected. Solid curve in Figure 3b shows the transmittance of the sample as a function of wavelength of *p*-polarized fundamental radiation, which incidents at 35°. A sharp peak which is observed around 765 nm is associated with a TPP. Measured intensity of the *p*-polarized SH radiation is represented by dots. It peaks at the same angle of incidence exceeding the out-of-resonance background by a factor of 300. Purple triangles show the intensity of SH from bare silver film, measured at the same pump power. Magnitude of the SH, generated in a sample in comparison with a bare silver film is significantly higher (120-fold in the maximum of TPP resonance).

Numerical calculations with a nonlinear transfer matrix technique were performed, using realistic dielectric constants of sample materials and assuming that the only source of nonlinearity is a 2-nm-thick layer of silver, adjacent to the interface with a PC. Result is shown in Figure 3b with a dashed line. It coincides well with experimental data, and small discrepancy could be explained assuming the finite width of laser spectrum as well as angular divergence of the fundamental beam.

3.2 Case of a double-resonance heterostructure

As it was mentioned earlier, in a typical photonic crystal/metal system, consisting of pairs of quarter-wavelength layers, wavelength λ_{T3} of TPP resonance in the third-order bandgap is not exactly one-third of the wavelength λ_T of the TPP resonance in fundamental bandgap due to nonlinear law of dispersion for materials of layers. However, in a heterostructure $(ABA^*B^*)_n Me$ comprising pairs of quarter-wavelength-thick layers (AB)

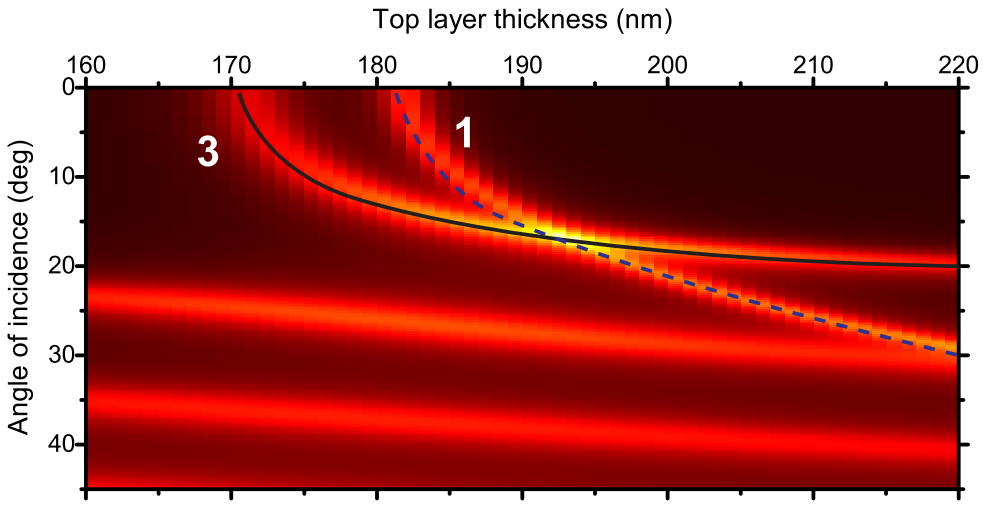

Figure 4. (Color online) Map of the designed heterostructure transmittance versus the angle of incidence and thickness of the topmost layer of a PC. Dashed and solid curves are guides for the eye and represent law of dispersion for fundamental (1560 nm) and third-order (520 nm) TPP resonance respectively. Bright lines in the bottom part of graph are third-order waveguide modes of a PC.

and pairs of layers with adjusted thicknesses (A*B*), condition $3\lambda_{T3} = \lambda_T$ can be fulfilled at some particular angle of incidence. For the experimental study of the THG enhancement, a sample of a heterostructure $\{[(SiO_2/Ta_2O_5)(SiO_2/Ta_2O_5)^*]_5/Ag/Al_2O_3\}$ was manufactured and characterized using scanning electron microscopy and transmittance spectroscopy. According to the results of measurements, the sample has the following average thicknesses of layers: 164 nm (Ta_2O_5), 194 nm (Ta_2O_5*), 240 nm (SiO_2), 284 nm (SiO_2*), 30 nm (Ag), and 10 nm (Al_2O_3). Parameters of the photonic crystal layers should be chosen and monitored precisely in order to fulfill the double-resonance conditions, because rather small variation in layer thickness can destroy them. In order to verify whether those conditions were satisfied in experiment or not, the numerical calculations were performed using a nonlinear transfer matrix technique, which allows for simulating both linear and nonlinear optical response of layered structures. Parameters of a model sample were taken from results of a manufactured sample characterization. Because spectral and angular position of a TPP resonance is the most sensitive to the thickness of the topmost layer of a PC (d_{top}), it was chosen as a model parameter and varied around the experimentally measured value. Figure 4 shows calculated dependences of a sample transmission on the angle of incidence and d_{top} at fundamental (1560 nm) and third-harmonic (520 nm) wavelength overlaid. Two curves, the dashed and the solid one, are guides for the eye and indicate behavior of the fundamental and third-harmonic TPP mode respectively. They cross at $d_{top} = 194$ nm and $\theta = 18°$, i.e. in a sample with a given thickness of the topmost layer of a PC, third-order TPP resonance wavelength is exactly one-third of a fundamental TPP resonance wavelength at the angle of incidence of 18°.

In contrast with second-harmonic, third-harmonic generation is allowed in bulk centrosymmetric media, thus contributions from each sample layer should be considered. Calculated TH intensity versus angle of incidence and thickness of the topmost layer of a photonic crystal in *pp* combination of fundamental and third-harmonic polarizations is shown in Figure 5. As in Figure 4, dashed curve indicates law of dispersion of a fundamental TPP mode. Third-harmonic intensity along the whole fundamental curve is enhanced in comparison to the nonresonant regions because of pump field localization in sample. However, in the region where fundamental TPP resonance overlaps with the third-order one (intersection of solid and dashed curves), intensity of third harmonic is approximately two orders of magnitude bigger then outside of it. Thickness of the topmost layer of a PC at which the overlapping and enhancement occurs match the one, measured in the prepared sample.

4. CONCLUSIONS

In conclusion, the explicit evidences of the resonant second-harmonic generation enhancement in photonic crystal/metal structure in the presence of Tamm plasmon-polaritons are presented. It is shown that enhancement

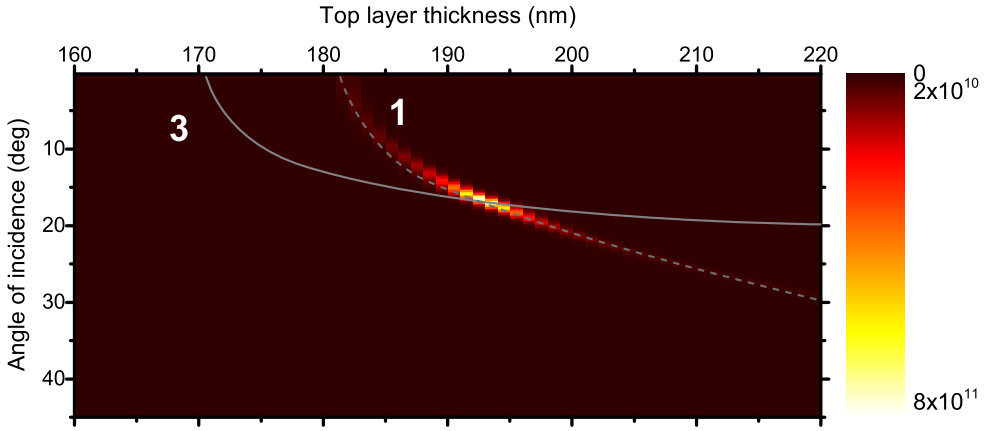

Figure 5. (Color online) Plot of the TH intensity, generated in a transmission geometry in *pp* combination of fundamental and TH radiation polarizations, versus the angle of incidence and thickness of the topmost layer of a PC. Dashed and solid curves are the same as in Figure 4 and represent laws of dispersion of fundamental and third-harmonic TPP respectively.

factor in comparison to a bare metal film has a value of several hundreds for a case when fundamental radiation is in resonance with a TPP. It is verified numerically that dielectric heterostructures can be constructed to support resonances on both fundamental and higher harmonics frequencies and optical harmonics intensity in that case is enhanced over four orders of magnitude in comparison to a bare metal film. Calculations have also proven that the manufactured sample has the optimal parameters for resonance overlapping, which motivates future experimental study of the phenomenon. These results can be useful to improve sensing and probing of buried interfaces as well as to increase efficiency of structures with active layers under the metal film.

5. ACKNOWLEDGMENTS

This work was supported by Russian Foundation for Basic Research (RFBR) (numerical calculations) and Russian Science Foundation (RSF) (experimental measurements) (15-02-00065).

REFERENCES

[1] Williams, C. T. and Beattie, D. A., "Probing buried interfaces with non-linear optical spectroscopy," *Surface Science* **500**(13), 545 – 576 (2002).

[2] Campagnola, P. J., Clark, H. A., Mohler, W. A., Lewis, A., and Loew, L. M., "Second-harmonic imaging microscopy of living cells," *Journal of Biomedical Optics* **6**(3), 277–286 (2001).

[3] Nakayama, Y., Pauzauskie, P. J., Radenovic, A., Onorato, R. M., Saykally, R. J., Liphardt, J., and Yang, P., "Tunable nanowire nonlinear optical probe," *Nature* **447**(7148), 1098–1101 (2007).

[4] Kim, S., Jin, J., Kim, Y.-J., Park, I.-Y., Kim, Y., and Kim, S.-W., "High-harmonic generation by resonant plasmon field enhancement," *Nature* **453**(7196), 757–760 (2008).

[5] Hubert, C., Billot, L., Adam, P.-M., Bachelot, R., Royer, P., Grand, J., Gindre, D., Dorkenoo, K. D., and Fort, A., "Role of surface plasmon in second harmonic generation from gold nanorods," *Applied Physics Letters* **90**(18), 181105 (2007).

[6] Soboleva, I., Murchikova, E., Fedyanin, A., and Aktsipetrov, O., "Second-and third-harmonic generation in birefringent photonic crystals and microcavities based on anisotropic porous silicon," *App. Phys. Lett.* **87**, 241110 (2005).

[7] Corcoran, B., Monat, C., Grillet, C., Moss, D. J., Eggleton, B. J., White, T. P., O'Faolain, L., and Krauss, T. F., "Green light emission in silicon through slow-light enhanced third-harmonic generation in photonic-crystal waveguides," *Nat. Photonics* **3**(4), 206–210 (2009).

[8] Gaspar-Armenta, J. A. and Villa, F., "Photonic surface-wave excitation: photonic crystal–metal interface," *J. Opt. Soc. Am. B* **20**(11), 2349–2354 (2003).

[9] Sasin, M. E., Seisyan, R. P., Kalitteevski, M. A., Brand, S., Abram, R. A., Chamberlain, J. M., Egorov, A. Y., Vasil'ev, A. P., Mikhrin, V. S., and Kavokin, A. V., "Tamm plasmon polaritons: Slow and spatially compact light," *App. Phys. Lett.* **92**(25), 251112 (2008).

[10] Kaliteevski, M., Iorsh, I., Brand, S., Abram, R. A., Chamberlain, J. M., Kavokin, A. V., and Shelykh, I. A., "Tamm plasmon-polaritons: Possible electromagnetic states at the interface of a metal and a dielectric bragg mirror," *Phys. Rev. B* **76**, 165415 (2007).

[11] Brückner, R., Sudzius, M., Hintschich, S. I., Fröb, H., Lyssenko, V. G., and Leo, K., "Hybrid optical tamm states in a planar dielectric microcavity," *Phys. Rev. B* **83**, 033405 (2011).

[12] Symonds, C., Lemaître, A., Homeyer, E., Plenet, J. C., and Bellessa, J., "Emission of tamm plasmon/exciton polaritons," *App. Phys. Lett.* **95**(15), 151114 (2009).

[13] Braun, T., Baumann, V., Iff, O., Hfling, S., Schneider, C., and Kamp, M., "Enhanced single photon emission from positioned inp/gainp quantum dots coupled to a confined tamm-plasmon mode," *Applied Physics Letters* **106**(4), 041113 (2015).

[14] Afinogenov, B. I., Bessonov, V. O., Nikulin, A. A., and Fedyanin, A. A., "Observation of hybrid state of tamm and surface plasmon-polaritons in one-dimensional photonic crystals," *Applied Physics Letters* **103**(6), 061112 (2013).

[15] Brückner, R., Zakhidov, A., Scholz, R., Sudzius, M., Hintschich, S., Fröb, H., Lyssenko, V., and Leo, K., "Phase-locked coherent modes in a patterned metal-organic microcavity," *Nature Photonics* **6**, 322–326 (2012).

[16] Lheureux, G., Azzini, S., Symonds, C., Senellart, P., Lematre, A., Sauvan, C., Hugonin, J.-P., Greffet, J.-J., and Bellessa, J., "Polarization-controlled confined tamm plasmon lasers," *ACS Photonics* **2**(7), 842–848 (2015).

[17] Liew, T. C. H., Kavokin, A. V., Ostatnický, T., Kaliteevski, M., Shelykh, I. A., and Abram, R. A., "Exciton-polariton integrated circuits," *Phys. Rev. B* **82**, 033302 (2010).

[18] Lee, K. J., Wu, J. W., and Kim, K., "Enhanced nonlinear optical effects due to the excitation of optical tamm plasmon polaritons in one-dimensional photonic crystal structures," *Opt. Express* **21**(23), 28817–28823 (2013).

[19] Lu, W., Xie, P., Zhang, Z.-Q., Wong, G. K. L., and Wong, K. S., "Simultaneous perfect phase matching for second and third harmonic generations in zns/yf3 photonic crystal for visible emissions," *Opt. Express* **14**(25), 12353–12358 (2006).

[20] Afinogenov, B. I., Bessonov, V. O., and Fedyanin, A. A., "Second-harmonic generation enhancement in the presence of tamm plasmon-polaritons," *Opt. Lett.* **39**(24), 6895–6898 (2014).